

XMM-NEWTON OBSERVATIONS OF RADIO PULSARS B0834+06 AND B0826–34 AND IMPLICATIONS FOR THE PULSAR INNER ACCELERATOR

J. GIL,¹ F. HABERL,² G. MELIKIDZE,^{1,3} U. GEPPERT,⁴ B. ZHANG,⁵ AND G. MELIKIDZE, JR.¹

Received 2008 April 2; accepted 2008 May 31

ABSTRACT

We report the X-ray observations of two radio pulsars with drifting subpulses, B0834+06 and B0826–34, using *XMM-Newton*. PSR B0834+06 was detected with a total of 70 counts from the three EPIC instruments over 50 ks exposure time. Its spectrum is best described as that of a blackbody (BB), with temperature $T_s = (2.0^{+2.0}_{-0.9}) \times 10^6$ K and bolometric luminosity $L_b = (8.6^{+14.2}_{-4.4}) \times 10^{28}$ erg s⁻¹. As is typical in pulsars with BB thermal components in their X-ray spectra, the hot-spot surface area is much smaller than that of the canonical polar cap, implying a non-dipolar surface magnetic field much stronger than the dipolar component derived from the pulsar spin-down (in this case about 50 times smaller and stronger, respectively). The second pulsar, PSR B0826–34, was not detected over the 50 ks exposure time, giving an upper limit for the bolometric luminosity $L_b \leq 1.4 \times 10^{29}$ erg s⁻¹. We use these data, as well as the radio emission data concerned with drifting subpulses, to test the partially screened gap (PSG) model of the inner accelerator in pulsars. This model predicts a simple and very intuitive relationship between the polar cap thermal X-ray luminosity (L_b) and the “carousel” period (P_4) for drifting subpulses detected in the radio band. The PSG model has been previously successfully tested with four radio pulsars whose L_b and P_4 were both measured: PSR B0943+10, PSR B1133+16, PSR B0656+14, and PSR B0628–28. The *XMM-Newton* X-ray data of PSR B0834+16 reported here are also in agreement with the model prediction, and the upper limit derived from the PSR B0826–34 observation does not contradict it. We also include two other pulsars, PSR B1929+10 and B1055–52, whose L_b and/or P_4 data became available just recently. These pulsars also follow the prediction of the PSG model. The clear prediction of the PSG model is now supported by all pulsars whose L_b and P_4 are measured and/or estimated.

Subject headings: pulsars: individual (B0834+06, B0826–34) — radiation mechanisms: thermal — stars: neutron — X-rays: stars

1. INTRODUCTION

More than 40 years after the discovery of radio pulsars, the mechanism by which they emit coherent radio beams is still not fully understood. Also, many properties of this radiation remain a mystery, especially the phenomenon of drifting subpulses, which is widely regarded as a powerful tool for the investigation of the pulsar radiation mechanism. Recently, this phenomenon has received renewed attention, mostly owing to newly developed techniques for the analysis of pulsar radio emission fluctuations (Edwards & Stappers 2002, 2003). Using these techniques, Weltevrede et al. (2006a, 2006b, hereafter W06a, W06b) presented results of a systematic, unbiased search for the drifting subpulses and/or phase-stationary intensity modulations in single pulses of a large sample of pulsars. They found that the fraction of pulsars showing evidence of drifting subpulses is at least 60%, and concluded that the conditions necessary for the drifting mechanism to work cannot be very different from the emission mechanism of radio pulsars.

It is therefore likely that the drifting-subpulse phenomenon originates from the so-called inner acceleration region right above the polar cap, which powers the pulsar radiation. In the classical model of Ruderman & Sutherland (1975), the subpulse-associated spark filaments of plasma circulate in the pure vacuum gap (VG) around the magnetic axis due to the well-known drift of plasma with non-corotational charge density (see the Appendix for more details).

There are a few periodicities characteristic for this model, also called the pulsar carousel model: the primary period P_3 , which can be measured as a distance between the observed subpulse drift bands, the secondary period (apparent when drifting is aliased; see Gil & Sendyk 2003 for a detailed description), and the tertiary period P_4 (also called the carousel time,⁶ as it is the time interval during which the gap plasma completes one full circulation around the magnetic pole). The carousel model is widely regarded as a natural and qualitative explanation of the drifting-subpulse phenomenon. However, its original version, published by Ruderman & Sutherland (1975, hereafter RS75), predicts too high a drifting rate for the sparks around the polar cap, as compared with the observations of drifting subpulses (e.g., Deshpande & Rankin 1999, 2001), and too high a heating rate of the polar cap (PC) surface due to the spark-associated back-flow bombardment, as compared with X-ray observations (e.g., Zhang et al. 2000). Another difficulty of the RS75 model is that recent calculations strongly suggest that the surface binding energies of both ions and electrons are too low to allow the development of a vacuum gap. Indeed, when the surface magnetic field is purely dipolar, then the gap can develop only in magnetars and several of the highest B -field pulsars (Medin & Lai 2007, hereafter ML07). Another type of inner accelerator model, called space-charge limited flow (SCLF; Arons & Scharlemann 1979; Harding & Muslimov 1998), has been discussed in the literature, and assumes that both ions and electrons can be freely stripped off the neutron star surface. Although this approximation is valid for most pulsars assuming a pure dipolar field at the polar cap region, a stronger,

¹ J. Kepler Institute of Astronomy, University of Zielona Góra, Poland.

² Max Planck Institute for Extraterrestrial Physics, Garching, Germany.

³ E. Kharadze Georgian National Astrophysical Observatory, Tbilisi, Georgia.

⁴ German Aerospace Center, Institute for Space Systems, Berlin, Germany.

⁵ Department of Physics, University of Nevada, Las Vegas, NV 89154.

⁶ Designated as \hat{P}_3 in RS75. Although this symbol is still in use, we advocate to replace it by P_4 .

TABLE 1
THERMAL X-RAY RADIATION FOR A HOT POLAR CAP IN PULSARS WITH DRIFTING SUBPULSES

PSR	P (s)	\dot{P}_{-15}	\dot{E} (erg s ⁻¹)	P_4/P	Ref.	L_b (erg s ⁻¹)	Ref.	L_b/\dot{E}	T_s (10 ⁶ K)
B0943+10.....	1.09	3.49	1.0×10^{32}	$37.4^{+0.4}_{-1.4}$	1	$(5.0^{+0.6}_{-1.7})10^{28}$	9	$(0.49^{+0.06}_{-0.16})10^{-3}$	$3.1^{+0.9}_{-1.1}$
B1133+16.....	1.19	3.73	8.8×10^{31}	33 ± 3	2				
				32 ± 4	3	$(6.8^{+1.1}_{-1.3})10^{28}$	10	$(0.77^{+0.13}_{-0.15})10^{-3}$	$3.2^{+1.9}_{-1.0}$
B0834+06.....	1.27	6.8	1.3×10^{32}	30.2 ± 0.2	4	$(8.6^{+14.2}_{-4.4})10^{28}$	5	$(0.67^{+1.1}_{-0.6})10^{-3}$	$2.0^{+2.0}_{-0.9}$
B1929+10.....	0.23	1.16	3.9×10^{33}	50^{+15}_{-5}	5	$(1.17^{+0.13}_{-0.4})10^{30}$	11	$(0.29^{+0.04}_{-0.09})10^{-3}$	$3.5^{+0.2}_{-0.5}$
B0656+14.....	0.38	55.0	3.8×10^{34}	20 ± 1	6	$(5.7^{+0.6}_{-0.8})10^{31}$	12	$(1.5 \pm 0.3)10^{-3}$	$1.25^{+0.03}_{-0.03}$
B1055-52.....	0.19	5.8	3.0×10^{34}	22^{+11}_{-5}	7	$(1.6^{+0.88}_{-0.42})10^{31}$	12	$(0.53^{+0.88}_{-0.42})10^{-3}$	$1.8^{+0.06}_{-0.06}$
B0628-28.....	1.24	7.12	1.5×10^{32}	7 ± 1	6	$(2.9^{+1.5}_{-0.8})10^{30}$	13	$(1.9^{+1.0}_{-0.5})10^{-2}$	$3.3^{+1.3}_{-0.6}$
B0826-34.....	1.85	0.99	6.2×10^{30}	14 ± 1	8	$<1.45 \times 10^{29}$	5	$<2.2 \times 10^{-2}$	

NOTE.—Errors in L_b and T_s correspond to a 2 σ (90% confidence) level.

REFERENCES.—(1) Deshpande & Rankin 1999; (2) Paper I; (3) HR07; (4) RW07; (5) this paper; (6) Paper II; (7) Biggs (1990); (8) Gupta et al. 2004; (9) Zhang et al. 2005; (10) Kargaltsev et al. 2006; (11) M07; (12) DL05; (13) Tepedelenlioglu & Ögelman 2005.

multipole magnetic field near the polar cap region (which is needed to raise a large number of radio pulsars above the radio emission death line; RS75; Zhang et al. 2000) would introduce a non-negligible binding energy for ions and electrons (ML07), which would render the SCLF approximation no longer valid. Another difficulty of the steady state SCLF model widely discussed in the literature is that it does not predict the existence of any “sparks” that could give rise to the drifting subpulses. Therefore, in our opinion, it is not an attractive inner accelerator model for interpreting pulsar radio emission.

Motivated by these shortcomings of the otherwise attractive VG model, Gil et al. (2003, hereafter G03) further developed the idea of the inner acceleration region above the polar cap by including the partial screening caused by the thermionic flow of ions from the PC surface heated by sparks. We call this kind of inner acceleration region a “partially screened gap” (PSG). The PSG is thermally self-regulated in such a way that the surface temperature is always close to, but slightly lower (by less than 1%) than, the critical temperature at which the maximum corotational ion outflow occurs, and thus the gap is fully screened (see the Appendix and/or G03 for more details). Moreover, if the surface temperature were even few percent lower than the critical temperature, there would be a pure vacuum gap, with all the problems discussed above. Since the actual potential drop in the PSG is much lower than that of the pure VG model (RS75), the intrinsic drift rate and PC heating rate are compatible with measurements of P_4 and L_b , respectively.

The PSG model can be tested if two observational quantities are known: (1) the circulatory period P_4 for drifting subpulses observed in radio emission and (2) the X-ray bolometric luminosity L_b of thermal blackbody (BB) radiation from the hot polar cap (see the Appendix). Radio pulsars have been targeted since the beginning of X-ray astronomy for various scientific reasons. Zhang et al. (2005) were the first to make an attempt to resolve the mystery of drifting subpulses in radio pulsars by observing them in X-rays. They proposed to detect thermal X-ray photons from the PC heated by sparks of plasma likely to be associated with drifting subpulses observed in the radio band. Their choice was the best-studied drifting-subpulse pulsar B0943+10. Using the *XMM-Newton* X-ray observatory, they detected a weak source coincident with the target pulsar. Due to the very small number of counts detected, no unambiguous spectrum could be obtained. However, they were able to fit the BB model to the data, although a power-law model was acceptable as well. Within a BB model, they inferred a bolometric luminosity $L_b \sim 5 \times 10^{28}$ erg s⁻¹ emitted from the hot spot (a few MK) with a surface area much smaller (by about 60 times)

than the conventional polar cap area as defined by the bundle of last-closed dipolar field lines. This radio pulsar was well studied by Deshpande & Rankin (1999), who described the number of sparks and the circulation time $P_4 = 37.4P$ needed for one full revolution around the pole (where P is the basic pulsar period). These properties also could not be accounted for by the conventional theory, and some radical modification of the RS75 model was required. It appears that the PSG model not only resolves all the problems of the RS75 model, but also offers a clean prediction that can be used to test theories of the inner pulsar accelerator.

2. PREVIOUS WORK

Gil et al. (2006, hereafter Paper I) reanalyzed the B0943+10 case within the PSG model. They derived a very useful formula directly connecting the drifting rate of plasma sparks (measured by the circulation period P_4) and the polar cap heating rate by back-flow spark bombardment (measured by the bolometric thermal luminosity L_b). By assuming that both measured quantities are determined by the same value of electric field in the PSG, they obtained a simple formula relating the so-called efficiency of thermal radiation from the hot polar cap to the circulation time:

$$L_b/\dot{E} = 0.63(P_4/P)^{-2}, \quad (1)$$

where \dot{E} is the pulsar spin-down (see eq. [A3] with $I_{45} = \alpha = 1$ in the Appendix). PSR B0943+10 (see data in Table 1) fitted this observational curve quite well (Fig. 1). When one observable parameter in equation (1) is known (L_b or P_4), the other one can be predicted without any free parameters. In Paper I, we included B1133+16, the twin pulsar to B0943+10 (at least in the sense of their kinematical properties; see Table 1). In this second case, we speculated that the long periodicity of about $30P$ revealed by a number of authors (e.g., W06a, W06b) is actually the circulatory period $P_4 \sim 30P$. This claim was recently confirmed by the sophisticated data analysis of Herfindal & Rankin (2007, hereafter HR07), although these authors admitted that they did not believe our prediction for the value of P_4 before they had done their own analysis. The X-rays from B1133+16 were detected using the *Chandra* X-ray observatory by Kargaltsev et al. (2006), who found that the pulsar’s properties were similar to those of its twin pulsar B0943+10. Because of the small number of counts detected, obtaining a unique spectrum was not possible, as in the case of PSR B0943+10 (Zhang et al. 2005). However, the BB model was acceptable and gave a bolometric luminosity $L_b \sim 3 \times 10^{28}$ erg s⁻¹ emitted from the hot (a few MK) and very small

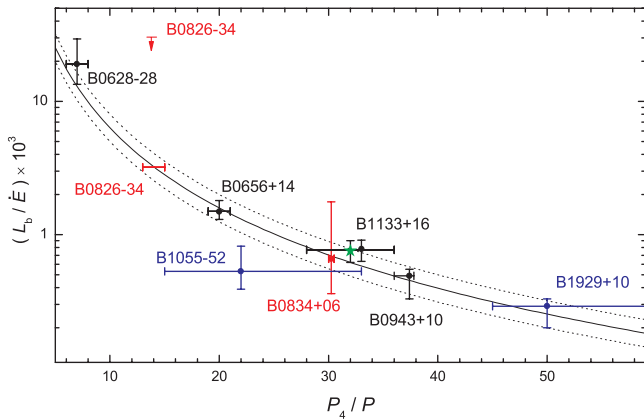


FIG. 1.—Efficiency of thermal X-ray emission from a hot polar cap L_b/\dot{E} vs. circulation period P_4 of drifting subpulses in the radio band. The solid curve represents the prediction of the PSG model (eq. [1]), while the dotted curves correspond to uncertainties in determining the moment of inertia (see the Appendix). The values of P_4 and L_b , along with their error bars (2σ) and references for the data, are given in Table 1.

polar cap (again much smaller—by about 100 times—than the canonical one). As one can see in Figure 1, with the inferred values of P_4 and L_b , the pulsar B1133+16 nicely clusters with its twin along the critical curve expressed by equation (1). Note that the filled circle for B1133+16 represents our prediction and the green star represents the estimate of P_4 by HR07.

Encouraged by the observational confirmation of our prediction of P_4 in B1133+16, we applied the same method to two other pulsars for which the measurements or estimates of thermal bolometric luminosity were available (Gil et al. 2007, hereafter Paper II). One of the famous Three Musketeers, PSR B0656+14, in which thermal X-rays from a small hot polar cap were clearly detected by De Luca et al. (2005, hereafter DL05), was an obvious choice. The BB thermal luminosity $L_b \sim 5.7 \times 10^{31}$ ergs s⁻¹ (Table 1), when inserted into equation (1), returned the predicted value of $P_4 = 20.6P$. Amazingly, Weltevrede et al. (2006b) reported a long-period fluctuation spectral feature $(20 \pm 1)P$ associated with the quasi-periodic amplitude modulation of erratic and strong radio emission detected from this pulsar. Thus, it was tempting to interpret this period as the circulation time P_4 . With the values of P_4 and L_b shown above, pulsar B0656+14 fits equation (1) quite well (Fig. 1). Although the drifting subpulses were not apparent in this case, the erratic radio emission reported by Weltevrede et al. (2006b) was similar to the so-called Q-mode in PSR B0943+10 (showing clearly drifting subpulses in the organized B-mode). The low-frequency feature in the fluctuation spectra, identical to that of the B-mode, was found by Rankin & Suleymanova (2006; see their Fig. 6). Asgekar & Deshpande (2001) also detected this feature in the 35 MHz observations of PSR B0943+10 (see their Figs. 1 and 2). This simply means that the carousel plasma drift is maintained in both regular drifting and erratic (with no drifting subpulses) pulsar emission modes. This is a property of plasma and magnetic field interaction in the gap rather than the structure of this plasma. However, drifting subpulses can be clearly observed only if the gap plasma has some lateral structure, e.g., localized sparking discharges.

For the second of the Three Musketeers, PSR B1055-52, we have just found evidence of a low-frequency feature $f \sim 0.042$ cycles P^{-1} (Biggs 1990), which can be interpreted as the carousel periodicity $P_4/P \sim 22$. Using this interpretation, which was very fruitful in several other cases discussed above and below, we examine thermal X-ray radiation from the small hot spot de-

tected in this pulsar and attempt to test our PSG model in § 4.4. The third Musketeer (Geminga) is radio quiet, so although it shows thermal BB X-ray emission from the small hot spot, it is not useful for our analysis.

Another pulsar that we were able to examine using our method of inferring values of P_4 from intensity modulation spectra was PSR B0628-28. As indicated in Table 1, it was detected in X-rays by Tepedelenioğlu & Ögelman (2005) using *Chandra* and *XMM-Newton*. This was an exceptional pulsar (called “overluminous” by Becker et al. 2005) with an efficiency much larger than that of typical pulsars (Becker & Trümper 1997). For the thermal BB component alone, $L_b/\dot{E} \sim 1.9 \times 10^{-2}$ (Table 1). This value inserted to equation (1) gives the predicted value of $P_4 \sim (6 \pm 1)P$. Interestingly, Weltevrede et al. (2006b) reported for this pulsar a relatively short periodicity of $(7 \pm 1)P$ (Table 1). If this periodicity is interpreted as the circulation time P_4 , then this pulsar is not exceptional at all. It lies on the theoretical curve (eq. [1]) in Figure 1 at exactly the right place. PSR B0628-28 is just another (fourth) pulsar that satisfies the predictions of equation (1), which relates the efficiency of thermal X-ray radiation from a hot polar cap to the circulatory periodicity associated with drifting subpulses observed in radio emission.

In order to expand the sample of pulsars with measured/estimated values for both L_b and P_4 , we recently launched an observational campaign using the *XMM-Newton* observatory. We targeted two old pulsars with P_4 measurements but no previous X-ray observations. The two pulsars, PSR B0826-34 and PSR B0834+06, were observed during the *XMM-Newton* Cycles AO5 and AO6, respectively. Simultaneous radio monitoring was also performed, and we will report on these observations in a separate paper. PSR B0826-34 was not detected, although we have derived an upper limit for its thermal luminosity. We clearly detected PSR B0834+06, whose spectrum is best modeled by BB radiation from a small hot spot. We interpret this as being due to PC heating by back-flow bombardment, and have found that the bolometric L_b agrees well with the value predicted by equation (1) in the PSG model. For completeness, in this paper we include yet another pulsar, PSR B1929+10, whose bolometric thermal luminosity was recently determined by Misanovic et al. (2007, hereafter M07). We show that this pulsar also satisfies equation (1) by finding a suitable feature in the modulation spectra database of W06a and W06b (see § 4.3 for some details). The number of pulsars satisfying and/or consistent with equation (1) has thus increased to seven. To the best of our knowledge, no single counterexample exists. It is worth emphasizing that the only pulsars that can be used for this analysis are those for which both the bolometric luminosity L_b of thermal X-rays from a hot polar cap and the circulatory periodicity P_4 of drifting subpulses observed in the radio band are known. In our sample of 8 available cases, in 4 pulsars (B0656+14, B1055-52, B0834+06, and B1929+10⁷) small hot spots were clearly detected, while in 3 others, it is either possible to show evidence of hot-spot thermal emission (B1133+16 and B0628-28), or at least impossible to exclude such a component

⁷ Recently, Hui & Becker (2008) analyzed the same *XMM-Newton* data of B1929+10 (using a different method for data binning, resulting in better photon statistics per spectral bin) and argued that the hot BB component is statistically unjustified. However, if they allowed the BB radius and the temperature of the hot spot to be free parameters, then the best fit resulted in a very small hot-spot area, with a radius $r_b = 25.81^{+18.81}_{-25.81}$ m, perhaps even smaller than the one obtained by M07. In the opinion of Hui & Becker (2008), this is unacceptably small when compared to the canonical PC radius. However, within our model, this is the result of a relatively low dipolar surface magnetic field $B_d = 5 \times 10^{11}$ G. The actual non-dipolar magnetic field must be much higher (by about 400 times) to provide enough binding energy (ML07) for the creation of the PSG in this pulsar, which results in a hot-spot radius of $r_b = 300/20 = 15$ m (see § 5 for more details).

TABLE 2
XMM-Newton EPIC OBSERVATIONS OF PSR B0826–34 AND PSR B0834+06

POINTING DIRECTION		SATELLITE REVOLUTION	INSTRUMENT ^a	START TIME (UT)	END TIME (UT)	EXPOSURE ^b (ks)
R.A. (J2000.0)	Decl. (J2000.0)					
PSR B0826–34 (Obs. ID 0400020101)						
08 28 16.6.....	34 17 07	1269	pn	2006 Nov. 13 13:44:24	2006 Nov. 14 09:19:30	38.83
			MOS1	2006 Nov. 13 13:22:03	2006 Nov. 14 09:19:35	...
			MOS2	2006 Nov. 13 13:22:03	2006 Nov. 14 09:19:50	...
PSR B0834+06 (Obs. ID 0501040101)						
08 37 05.6.....	06 10 15	1454	pn	2007 Nov. 17 13:44:24	2007 Nov. 18 09:19:30	48.95
			MOS1	2007 Nov. 17 13:22:03	2007 Nov. 18 09:19:35	53.30
			MOS2	2007 Nov. 17 13:22:03	2007 Nov. 18 09:19:50	54.44

NOTE.—Units of right ascension are hours, minutes, and seconds, and units of declination are degrees, arcminutes, and arcseconds.

^a The three EPIC instruments were operated in full-frame CCD readout mode, with 73 ms frame time for pn and 2.6 s for MOS with thin optical blocking filters.

^b Net exposure times after background screening.

(B0943+10). The last case (B0826–34) is uncertain, as we only have an upper limit for X-ray detection (consistent with the PSG model).

3. NEW X-RAY DATA

We have observed two radio pulsars with the *XMM-Newton* observatory (Jansen et al. 2001), B0834+06 and B0826–34, known for their prominent subpulse drift. They are shown in red in Figure 1 to distinguish them from the four pulsars previously analyzed in Papers I and II (shown in black). Yet another pulsar, B1929+10, (shown in blue in Fig. 1) is discussed in § 4.3, as its values of L_b and P_4 have recently become available.

3.1. PSR B0834+06

The pulsar PSR B0834+06 was observed with *XMM-Newton* on 2007 November 17 and 18 for a total of ~ 71.7 ks. The EPIC MOS (Turner et al. 2001) and EPIC pn (Strüder et al. 2001) cameras were operated in imaging mode (see Table 2). The observation was scheduled at the end of the satellite revolution, and the detector background strongly increased when the satellite entered the radiation belts. To maximize the signal-to-noise ratio, we rejected the period of high background, which resulted in net exposure times of around 50 ks (Table 2).

For the X-ray analysis we used the *XMM-Newton* Science Analysis System (SAS), version 7.1.0, together with XSPEC, version 11.3.2p, for spectral modeling. Standard SAS source detection based on a maximum likelihood technique was simultaneously applied to the X-ray images obtained from the three EPIC instruments and five different energy bands (B1, 0.2–0.5 keV; B2, 0.5–1.0 keV; B3, 1.0–2.0 keV; B4, 2.0–4.5 keV; and B5, 4.5–12.0 keV). A weak source was found at the position of the pulsar at R.A. = $08^{\text{h}}37^{\text{m}}05.71^{\text{s}}$ and decl. = $06^{\circ}10'15.8''$ (J2000.0), with a 1σ statistical error of $1.7''$. Nearly 150 X-ray sources were detected in the EPIC images, and a comparison with catalogs from other wavelength bands yields many correlations within $\sim 0.5''$ of the X-ray positions. This demonstrates that the systematic uncertainty in the astrometry is small compared to the statistical error of the source position. The X-ray source position is within $1.3''$ of the radio position of PSR B0834+06, which is consistent within the errors. The positional agreement and other properties of the X-ray source (see below) make a chance coincidence very unlikely.

The total EPIC count rate (summed for the three instruments in the 0.2–4.5 keV band) obtained from the source detection analysis

is $(1.4 \pm 0.3) \times 10^{-3}$ counts s^{-1} , which is insufficient for a detailed spectral analysis. To obtain constraints on the shape of the X-ray spectrum, we therefore use hardness ratios (X-ray colors) derived from the count rates in the standard energy bands and compare them with those expected from various model spectra. Because the EPIC pn detector is more sensitive, in particular at low energies, where most of the counts are detected, we only use count rates obtained from EPIC pn. Hardness ratios are defined as $\text{HR1} = (R_2 - R_1)/(R_2 + R_1)$, $\text{HR2} = (R_3 - R_2)/(R_3 + R_2)$, $\text{HR3} = (R_4 - R_3)/(R_4 + R_3)$, and $\text{HR4} = (R_5 - R_4)/(R_5 + R_4)$, where R_N denotes the source count rate in band BN . To compare the measured hardness ratios with those inferred from model spectra, we simulated expected EPIC pn spectra (using XSPEC and the appropriate detector response files), and derived expected count rates and hardness ratios.

The distance to PSR B0834+06, estimated as 643 pc, was derived from its dispersion measure of $\text{DM} = 12.86$ pc cm^{-3} (from the online ATNF pulsar catalog).⁸ Assuming a 10% ionization degree of the interstellar matter along the line of sight to PSR B0834+06, this converts to a hydrogen column density of $N_{\text{H}} = 4.0 \times 10^{20}$ cm^{-2} . Because of the low statistical quality of the X-ray data, we are not able to derive tight constraints on the absorbing column density. Therefore, we limit our investigated model parameter space to N_{H} values between 1.0×10^{20} cm^{-2} (a lower limit reached within a distance of 200 pc; Posselt et al. 2008) and 8.0×10^{20} cm^{-2} (allowing an uncertainty of a factor of 2 in the assumed ionization degree for the conversion from DM to N_{H}).

As model spectra, we tested power-law (PL) and blackbody (BB) emission, and a combination of the two. In all model spectra, absorption was included, assuming elemental abundances from Wilms et al. (2000). For the absorbed power-law model, we explored the parameter space for N_{H} between 1.0×10^{20} and 8.0×10^{20} cm^{-2} , with a step size of 1.0×10^{20} cm^{-2} , and with a photon index γ between 1 and 5 in steps of 0.2. Figure 2a shows the hardness ratios HR1 versus HR2 derived at the parameter grid points. The measured hardness ratios HR1 and HR2 are drawn with 1σ (solid lines) and 2σ (dotted lines) error bars. The rectangular boxes around the error bars indicate the corresponding confidence areas, although in reality these are limited by error ellipses that fit inside the boxes. As can be seen, the power-law model spectra cannot reproduce the measured hardness ratios within the

⁸ See <http://www.atnf.csiro.au/research/pulsar/psrcat/>.

The cohesive energy calculations of Fe ion chains in an ultrastrong magnetic field by ML07 seem to be strongly supported by the X-ray observations discussed in this paper.

Finally, we would like to address a hypothesis put forward by Becker et al. (2006) that in old pulsars ($>10^6$ yr), the magnetospheric emission dominates over thermal emission, including both cooling radiation and hot polar cap emission components. These authors suggested that the latter radiation component decreases along with the former one, and therefore that the hot polar caps in cooling neutron stars could be formed by anisotropic heat flow due to the presence of the magnetic field rather than by particle bombardment. While in young neutron stars with core temperatures $\simeq 10^8$ K, the strong crustal magnetic fields may channel the heat toward the polar cap, resulting in a T_s of a few MK (Perez-Azorin et al. 2006; Geppert et al. 2006), in pulsars older than 10^6 yr this mechanism is much less efficient, and the only viable process that can produce such hot and small polar caps is back-flow particle bombardment. Almost all pulsars presented and examined in this paper are older than 1 Myr (an exception is the 110 kyr PSR B0656+14). For instance, PSR B0834+06 is 3 Myr old, and its X-ray emission is dominated by the hot BB component (a counterexample to Becker et al. 2006). In PSR B1929+10 (3.1 Myr old), the luminosity of the hot BB component is at least comparable to the magnetospheric X-ray radiation (M07). The very old (170 Myr) rotation-powered non-recycled pulsar J0108-1431 clearly shows BB radiation from the hot polar cap (Pavlov et al. 2008), which is probably accompanied by magnetospheric emission, although there is no evidence of cooling radiation from the whole surface, as expected for such an old pulsar.

In summary, both the polar cap full cascade (Zhang & Harding 2000) and the downward outer gap cascade (Cheng et al. 1998), which have been proposed to interpret nonthermal X-ray emis-

sion from spin-down-powered pulsars, are expected to be less significant in pulsars from our sample than in young pulsars. The predicted values of X-ray luminosity in these models are typically lower than that of the polar cap heating in the PSG model (eq. [1]). As other available models of the pulsar inner accelerator (the pure vacuum gap model and the space-charge limited flow model) either overpredict or underpredict the polar cap heating level, we conclude that the pulsar inner accelerator is likely partially screened due to a self-regulated sub-Goldreich Julian flow. Also, the pure vacuum gap model predicts too fast a drifting, and the space-charge limited flow model has no natural explanation for the subpulse drift phenomenon. We thus strongly believe that thermal radiation associated with polar cap heating due to a partially screened inner accelerator is a common component of pulsar X-ray emission regardless of the pulsar's age, and that this component plays an especially significant role in the spectra of old pulsars.

Our results are partly based on observations made with *XMM-Newton*, an ESA science mission with instruments and contributions directly funded by ESA member states and the USA (NASA). We acknowledge the support of NASA grants NNX07AF07G and NNX08AC67G. J. G. was partially supported by the Polish State Committee for Scientific Research grant NN203 2738 33, and G. M. was partially supported by the Polish State Committee for Scientific Research grant NN203 1262 33, as well as by the Georgian grants NSF ST06/4 096 and INTAS 06 1000017 9258. The *XMM-Newton* project is supported by the Bundesministerium für Wirtschaft und Technologie/Deutsches Zentrum für Luft und Raumfahrt (BMWi/DLR, FKZ 50 OX 0001) and the Max Planck Society. We thank Dipanjan Mitra for stimulating discussions, critical reading of the manuscript, and helpful comments.

APPENDIX

INNER ACCELERATION REGION IN PULSARS

The charge-depleted inner acceleration region above the polar cap results from the deviation of a local charge density ρ from the corotational charge density (Goldreich & Julian 1969) $\rho_{GJ} = -\Omega \cdot \mathbf{B}_s / 2\pi c \approx B_s / cP$. For isolated neutron stars, one might expect the surface to consist mainly of the iron formed at the neutron star's birth (e.g., Lai 2001). Therefore, the charge depletion above the polar cap could result from binding of the positive ^{56}Fe ions (at least partially) in the neutron star surface. If this is really possible (see Medin & Lai 2006, 2007 and Paper II for details), then the positive charges cannot be supplied at a rate that would compensate for the inertial outflow through the light cylinder. As a result, a significant part of the unipolar potential drop develops above the polar cap, which can accelerate positrons to relativistic energies and power the pulsar radiation mechanism, while the electrons bombard the polar cap surface, causing a thermal ejection of ions, which would otherwise be more likely bound in the surface in the absence of additional heating. This thermal ejection would cause partial screening of the acceleration potential drop ΔV , corresponding to a shielding factor $\eta = 1 - \rho_i / \rho_{GJ}$ (see G03 for details), where ρ_i is the charge density of the ejected ions, $\Delta V = \eta(2\pi/cP)B_s h^2$ is the potential drop, and h is the height of the acceleration region. The gap potential drop is completely screened when the total charge density $\rho = \rho_i + \rho_+$ reaches the corotational value ρ_{GJ} . In terms of the binding of ^{56}Fe ions, the screening factor $\eta = 1 - \exp(C_i - \varepsilon_c/kT_s)$, where ε_c is the cohesive energy of the condensed iron surface, T_s is the actual surface temperature, $T_i = \varepsilon_c/kC_i$ is the critical temperature above which the iron ions are ejected with the maximum corotation-limited rate, and $C_i = 30 \pm 3$ (ML07).

Because of the exponential sensitivity of the accelerating potential drop to the surface temperature, the actual potential drop should be thermostatically regulated. In fact, when the potential drop is large enough to ignite cascading pair production, the back-flowing relativistic charges will bombard the polar cap surface and heat it at a predictable rate. This heating will induce thermionic emission from the surface, which will, in turn, decrease the potential drop that caused the thermionic emission in the first place. As a result of these two oppositely directed tendencies, a quasi-equilibrium state should be established, in which heating due to electron bombardment is balanced by cooling due to thermal radiation. This should occur at a temperature slightly lower than the critical temperature above which the polar cap surface delivers thermionic flow at the corotational charge density level. This is the essence of the PSG model. For practical reasons, it is assumed that $T_s = T_i$, although in reality T_s is a few thousand K lower than T_i , the latter being strongly dependent on the surface magnetic field B_s . This is illustrated by Figure 7 in ML07, which was prepared for the pure VG model. The PSG model is realized along the red (for Fe) line in this figure, which shows that for a few MK surface temperatures, as suggested by X-ray observations of pulsar hot spots (see Paper II and references therein), the surface magnetic field must be close to 10^{14} G in all pulsars. For most pulsars, this is a much stronger field than that inferred from pulsar spin-down due to magnetic dipole radiation. Therefore, the surface magnetic

field in neutron stars must be dominated by crust-anchored non-dipolar magnetic anomalies. Such a strong and curved surface magnetic field is also necessary for development of the cascading pair production via curvature radiation (e.g., RS75; Gil & Melikidze 2002).

Several models proposed for generating pulsar radio emission based on the concept of vacuum gaps need radii of curvature of the surface magnetic field much smaller than the stellar radius (see, e.g., Gil et al. 2002). A possible way to generate such fields would be via currents in the neutron star crust (e.g., Urpin et al. 1986; Geppert et al. 2003). Mitra et al. (1999) examined the evolution of multipole components generated by currents in the outer crust. They found that mostly low-order multipoles contribute to the required small radii of curvature and that the structure of the surface magnetic field is not expected to change significantly during the radio pulsar lifetime.

The spark plasma inside the PSG must slowly drift with respect to the polar cap surface due to non-corotational charge density. This drift will manifest itself by observed subpulse drifting, provided that the spark arrangement is quasi-stable over timescales of hundreds of pulses or so. The deviation of the charge density from the corotational value generates an electric field $\Delta E = \Delta E_{\parallel} + \Delta E_{\perp}$ just above the polar cap surface. The parallel component causes acceleration of charged particles, while the perpendicular component participates in the subpulse drift. The tangential electric field at the polar cap boundary $\Delta E_{\parallel} = 0.5\Delta V/h = \eta(\pi/cP)B_s h$ (see Appendix A in G03 for details). Due to the $\Delta E \times B_s$ drift, the discharged plasma performs a slow circumferential motion around the magnetic axis (see the next paragraph) with velocity $v_d = c\Delta E_{\perp}/B_s = \eta\pi h/P$. The time interval to make one full revolution around the polar cap boundary is $P_4 \approx 2\pi r_p/v_d$. One then has

$$\frac{P_4}{P} = 2 \frac{r_p}{\eta h \alpha}, \quad (\text{A1})$$

where the coefficient $\alpha = \Delta E_{\perp}/\Delta E_{\parallel}$ should be close to unity. If the plasma above the polar cap is fragmented into filaments (sparks), which determine the intensity structure of the instantaneous pulsar radio beam, then in principle the circumferential periodicity P_4 can be measured/estimated from the pattern of the observed drifting subpulses (Deshpande & Rankin 1999; Gil & Sendyk 2003). In practice, P_4 is measured from the low-frequency features in the modulation spectra obtained from good-quality single-pulse data of pulsars with drifting subpulses. According to RS75, $P_4 = NP_3$, where N is the number of sparks contributing to the drifting-subpulse pattern observed in a given pulsar, and P_3 is the primary drift periodicity (the distance between the observed nonaliased subpulse drift bands).

The circumferential motion around the magnetic axis, as in RS75, holds only when the magnetic and the spin axes are almost parallel (an almost-aligned rotator, in which the line-of-sight trajectory is almost that of the circumferential tracks of sparks moving around the magnetic axis). Many pulsars with drifting subpulses indeed have a very broad profile characteristic of almost-aligned rotators (e.g., B0826–34 and B0818–41). Others, which are not broad-profile pulsars and show regular drifting, must have a very high impact angle, i.e., one grazing the emission beam. In such cases, one cannot exclude the almost-aligned geometry. In the more general (inclined) case, the spark trajectory does not have to be closed on the polar cap, as sparks should rather follow the trajectory of the line of sight projected onto the polar cap, being slightly late behind the star's rotation. However, observations of drifting subpulses in some pulsars do not support such a scenario, being consistent with the circumferential motion of the spark-associated subbeams of subpulse radiation, even if the pulsar is not an aligned rotator. Indeed, orderly drifting subpulses always demonstrate a systematic intensity modulation that either increases or decreases toward the pulse profile midpoint. Also, in pulsars with a more central cut of the line-of-sight trajectory, the subpulse drift is less apparent (or nonexistent), but a characteristic phase-stationary modulation of subpulse intensity modulation persists. These properties strongly suggest that sparks move on closed trajectories on the polar cap, although they do not have to be circular, as in the axially symmetric RS75 model, to the extent that in some of the detections of circumferential motion with a specified value of P_4 , periodicity is possible. A good example of such a pulsar with a central line-of-sight cut is B0834+06, which is discussed in this paper. Therefore, there must be some agency that makes sparks move across the line-of-sight projection on closed trajectories around the local magnetic pole instead of around the rotational pole, irrespective of the inclination and impact angles.

The quasi-equilibrium condition is $Q_{\text{cool}} = Q_{\text{heat}}$, where $Q_{\text{cool}} = \sigma T_s^4$ is the cooling power surface density by thermal radiation from the polar cap surface, $Q_{\text{heat}} = \gamma m_e c^3 n$ is the heating power surface density due to back-flow bombardment, $\gamma = e\Delta V/m_e c^2$ is the Lorentz factor, $n = n_{\text{GJ}} - n_i = \eta n_{\text{GJ}}$ is the number density of the back-flowing particles that deposit their kinetic energy at the polar cap surface, η is the shielding factor, n_i is the charge number density of the thermionic ions, $n_{\text{GJ}} = \rho_{\text{GJ}}/e = 1.4 \times 10^{11} b \dot{P}_{-15}^{0.5} P^{-0.5} \text{ cm}^{-3}$ is the corotational charge number density, and \dot{P}_{-15} is the time derivative of the period in 10^{-15} . It is straightforward to obtain an expression for the quasi-equilibrium surface temperature in the form $T_s = (2 \times 10^6 \text{ K})(\dot{P}_{-15}/P)^{1/4} \eta^{1/2} b^{1/2} h_3^{1/2}$ (Paper II), where $h_3 = h/10^3 \text{ cm}$, the parameter $b = B_s/B_d = A_{\text{pc}}/A_p$ (Gil & Sendyk 2000; ML07) describes the domination of the local actual surface magnetic field over the canonical dipolar component at the polar cap, and \dot{P}_{-15} is the normalized period derivative. Here, $A_{\text{pc}} = \pi r_{\text{pc}}^2$ and $A_p = \pi r_p^2$ are the canonical (RS75) and actual emitting surface areas, respectively, where r_{pc} and r_p are the canonical (RS75) and actual polar cap radii, respectively. Since the typical polar cap temperature is $T_s \sim 10^6 \text{ K}$ (Paper II), the actual value of b must be much larger than unity, as expected for highly non-dipolar surface magnetic fields.

Using equation (A1), one can derive the formula for thermal X-ray luminosity as

$$L_b = 2.5 \times 10^{31} \alpha^{-2} \left(\frac{\dot{P}_{-15}}{P^3} \right) \left(\frac{P_4}{P} \right)^{-2}, \quad (\text{A2})$$

or in a simpler form representing the radiation efficiency with respect to the spin-down power, $\dot{E} = I\Omega\dot{\Omega} = 3.95 I_{45} \times 10^{31} \dot{P}_{-15}/P^3 \text{ erg s}^{-1}$, where $I = I_{45} \times 10^{45} \text{ g cm}^2$ is the neutron star moment of inertia, and $I_{45} = 1_{-0.22}^{+1.25}$ (see Papers I and II for details). The equation

$$\frac{L_b}{\dot{E}} = 0.63 \left(\frac{\alpha^{-2}}{I_{45}} \right) \left(\frac{P_4}{P} \right)^{-2} \quad (\text{A3})$$

is very useful for direct comparison with observations, since it contains only the observed quantities (although it is subject to small uncertainty factors related to the unknown moment of inertia I_{45} and the coefficient α). It does not depend on any details of the sparking-gap model such as the non-dipolar surface magnetic field $b = B_s/B_d$, the height h of the acceleration region, or the shielding factor η , since they cancel out in the derivation procedure as expected. Indeed, this equation reflects the fact that both the subpulse drifting rate (due to the $\Delta E \times B_s$ plasma drift) and the polar cap heating rate (due to back-flow bombardment) are determined by the same physical quantity, which is the potential drop across the inner acceleration region just above the polar cap. No other agency should be involved. In a practical application of equation (A3), we will set $I_{45} = 1$ and $\alpha = 1$. The former is commonly used, and the latter means that the values of the accelerating E_{\parallel} and perpendicular E_{\perp} components of electric field in the PSG are almost the same. It is quite a reasonable assumption, all the more so since it seems to be supported observationally (Fig. 1).

REFERENCES

- Arons, J., & Scharlemann, E. T. 1979, *ApJ*, 231, 854
 Asgekar, A., & Deshpande, A. A. 2001, *MNRAS*, 326, 1249
 ———. 2005, *MNRAS*, 357, 1105 (AD05)
 Becker, W., Jessner, A., Kramer, M., Testa, V., & Howaldt, C. 2005, *ApJ*, 633, 367
 Becker, W., & Trümper, J. 1997, *A&A*, 326, 682
 Becker, W., et al. 2006, *ApJ*, 645, 1421
 Biggs, J. D. 1990, *MNRAS*, 246, 341
 Cheng, K. S., Gil, J., & Zhang, L. 1998, *ApJ*, 493, L35
 Cordes, J. M., & Lazio, T. J. W. 2002, preprint (astro-ph/0207156)
 De Luca, A., et al. 2005, *ApJ*, 623, 1051 (DL05)
 Deshpande, A. A., & Rankin, J. M. 1999, *ApJ*, 524, 1008
 ———. 2001, *MNRAS*, 322, 438
 Edwards, R. T., & Stappers, B. W. 2002, *A&A*, 393, 733
 ———. 2003, *A&A*, 407, 273
 Geppert, U., Küker, M., & Page, D. 2006, *A&A*, 457, 937
 Geppert, U., Rheinhardt, M., & Gil, J. 2003, *A&A*, 412, L33
 Gil, J., Lyubarsky, Y., & Melikidze, G. I. 2004, *ApJ*, 600, 872
 Gil, J., & Melikidze, G. I. 2002, *ApJ*, 577, 909
 Gil, J., Melikidze, G. I., & Geppert, U. 2003, *A&A*, 407, 315 (G03)
 Gil, J., Melikidze, G. I., & Mitra, D. 2002, *A&A*, 388, 235
 Gil, J., Melikidze, G., & Zhang, B. 2006, *A&A*, 457, L5 (Paper I)
 ———. 2007, *MNRAS*, 376, L67 (Paper II)
 Gil, J., & Sendyk, M. 2000, *ApJ*, 541, 351
 ———. 2003, *ApJ*, 585, 453
 Goldreich, P., & Julian, H. 1969, *ApJ*, 157, 869
 Gupta, Y., Gil, J., Kijak, J., & Sendyk, M. 2004, *A&A*, 426, 229
 Harding, A. K., & Muslimov, A. G. 1998, *ApJ*, 508, 328
 ———. 2001, *ApJ*, 556, 987
 ———. 2002, *ApJ*, 568, 862
 Herfindal, J. L., & Rankin, J. M. 2007, *MNRAS*, 380, 430 (HR07)
 Hui, C. Y., & Becker, W. 2008, *A&A*, 486, 485
 Jansen, F., et al. 2001, *A&A*, 365, L1
 Kargaltsev, O., Pavlov, G. G., & Garmire, G. P. 2006, *ApJ*, 636, 406
 Lai, D. 2001, *Rev. Mod. Phys.*, 73, 629
 Manchester, R. N., Hobbs, G. B., Teoh, A., & Hobbs, M. 2005, *AJ*, 129, 1993
 Medin, Z., & Lai, D. 2006, *Phys. Rev. A*, 74, 062507
 ———. 2007, *MNRAS*, 382, 1833 (ML07)
 Melikidze, G. I., Gil, J. A., & Pataraya, A. D. 2000, *ApJ*, 544, 1081
 Misanovic, Z., Pavlov, G. G., & Garmire, G. P. 2007, *ApJ*, submitted (arXiv:0711.4171) (M07)
 Mitra, D., Konar, S., & Bhattacharya, D. 1999, *MNRAS*, 307, 459
 Pavlov, G. G., Kargaltsev, O., Wong, J. A., & Garmire, G. P. 2008, *ApJ*, submitted (arXiv:0803.0761)
 Perez-Azorin, J. F., Miralles, J. A., & Pons, J. A. 2006, *A&A*, 451, 1009
 Posselt, B., Popov, S. B., Haberl, F., Trümper, J., Turolla, R., & Neuhäuser, R. 2008, *A&A*, 482, 617
 Rankin, J. M., & Suleymanova, S. A. 2006, *A&A*, 453, 679
 Rankin, J. M., & Wright, G. A. E. 2007, *MNRAS*, 379, 507 (RW07)
 Ruderman, M. A., & Sutherland, P. G. 1975, *ApJ*, 196, 51 (RS75)
 Strüder, L., et al. 2001, *A&A*, 365, L18
 Tauris, T. M., et al. 1994, *ApJ*, 428, L53
 Tepedelenlioglu, E., & Ögelman, H. 2005, *ApJ*, 630, L57
 Thorsett, S. E., & Chakrabarty, D. 1999, *ApJ*, 512, 288
 Turner, M. J. L., et al. 2001, *A&A*, 365, L27
 Urrin, V. A., Levshakov, S. A., & Iakovlev, D. G. 1986, *MNRAS*, 219, 703
 Weltevrede, P., Edwards, R. I., & Stappers, B. W. 2006a, *A&A*, 445, 243 (W06a)
 Weltevrede, P., Wright, G. A. E., Stappers, B. W., & Rankin, J. M. 2006b, *A&A*, 458, 269 (W06b)
 Wilms, J., Allen, A., & McCray, R. 2000, *ApJ*, 542, 914
 Xu, R. X., Qiao, G. J., & Zhang, B. 1999, *ApJ*, 522, L109
 Yue, Y. L., Cui, X. H., & Xu, R. X. 2006, *ApJ*, 649, L95
 Zhang, B., & Harding, A. K. 2000, *ApJ*, 532, 1150
 Zhang, B., Harding, A., & Muslimov, A. 2000, *ApJ*, 531, L135
 Zhang, B., Sanwal, D., & Pavlov, G. G. 2005, *ApJ*, 624, L109

